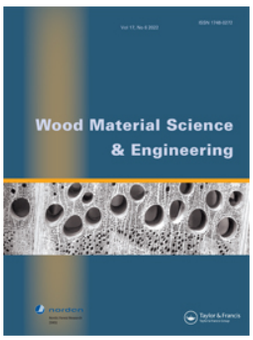

Wood Material Science & Engineering

ISSN: (Print) (Online) Journal homepage: https://www.tandfonline.com/loi/swoo20

Furfurylation of tropical wood species with and without silver nanoparticles: Part I: Analysis with confocal laser scanning microscopy and FTIR spectroscopy

Johanna Gaitán-Alvarez, Roger Moya, George I. Mantanis & Alexander Berrocal

To cite this article: Johanna Gaitán-Alvarez, Roger Moya, George I. Mantanis & Alexander Berrocal (2022) Furfurylation of tropical wood species with and without silver nanoparticles: Part I: Analysis with confocal laser scanning microscopy and FTIR spectroscopy, Wood Material Science & Engineering, 17:6, 410-419, DOI: 10.1080/17480272.2021.1886166

To link to this article: https://doi.org/10.1080/17480272.2021.1886166

Published online: 18 Feb 2021.

WOOD MATERIAL SCIENCE & ENGINEERING
2022, VOL. 17, NO. 6, 410–419
https://doi.org/10.1080/17480272.2021.1886166

Taylor & Francis
Taylor & Francis Group

ORIGINAL ARTICLE

Furfurylation of tropical wood species with and without silver nanoparticles: Part I: Analysis with confocal laser scanning microscopy and FTIR spectroscopy

Johanna Gaitán-Alvarez[a], Roger Moya[a], George I. Mantanis[b] and Alexander Berrocal[a]

[a]InstitutoTecnológico de Costa Rica, Escuela de Ingeniería Forestal, Cartago, Costa Rica; [b]Department of Forestry, Wood Sciences and Design, Laboratory of Wood Science and Technology, University of Thessaly, Karditsa, Greece

ABSTRACT

This work focused on the upgrading of non-durable tropical wood species originating from fast-growing plantations of Costa Rica. Modification of such tropical woods with furfuryl alcohol, although has not been broadly studied up to date, offers a potential way to increase their low durability. The purpose of this research was to investigate the modification effects on cell wall, vessels wall, radial and axial parenchyma using confocal laser scanning microscopy (CLSM) as well as the changes in the bands of chemical composition using Fourier-transform infrared spectroscopy (FTIR). In fact, nine tropical wood species such as *Cedrela odorata*, *Cordia alliodora*, *Enterolobium cyclocarpum*, *Gmelina arborea*, *Hieronyma alchorneoides*, *Samanea saman*, *Tectona grandis*, *Vochysia ferruginea* and *Vochysia guatemalensis* were treated with plain furfuryl alcohol (FA), and furfuryl alcohol combined with silver nanoparticles (FA-NPsAg). Furfurylation effects were also assessed by the weight percentage gain (WPG) of wood. Results showed that WPG varied from 14.4% to 44.3% with the FA treatment, and from 12.9% to 44.5% with the FA-NPsAg treatment. In the species which exhibited a WPG over 25% with the FA treatment, fluorescence at 600 nm band occurred mostly in the cell walls of fibres, while the furfurylation degree in radial and axial parenchyma was limited. Moreover, furfurylation occurred in lesser extent in wood species with high abundance of axial parenchyma as revealed by fluorescence. Wood species such as *Vochysia ferruginea, Vochysia guatemalensis, Cedrela odorata, Samanea saman*, *Enterolobium cyclocarpum*, which showed WPGs>25%, evidenced considerable changes in the lignin structure as observed in the FTIR spectra. In particular, with the FA treatment, the changes were observed in the bands of 1711, 1652, 1561, 889, 796 and 733 cm^{-1}, whereas, with the FA-NPsAg treatment, the changes occurred in the bands of 1711, 1505, 1426, 1370, 1224 and 1016 cm^{-1}. Overall, no significant difference was found in FTIR spectra and anatomical fluorescence between the FA and FA-NPsAg treatment, probably because the NPsAg concentration was insufficient for a change to occur in the bonds.

ARTICLE HISTORY
Received 20 November 2020
Revised 7 January 2021
Accepted 2 February 2021

KEYWORDS
Furfurylation; tropical species; silver nanoparticles; wood anatomical features

Introduction

Humans have used wood for thousands of years, because it is a natural, renewable material which is widely abundant and easy-to-work (Rowell 2012, Sandberg *et al*. 2017). Though wood has been utilised without any modification, this organic material has weaknesses such as low dimensional stability, and susceptibility to microorganisms (e.g. fungi, insects), which can cause its biodegradation. Consequently, several wood modification technologies have emerged thermal, chemical, and impregnation modification (Hill 2006, Rowell *et al*. 2009, Rowell 2012, Gérardin 2016, Sandberg *et al*. 2017, Papadopoulos *et al*. 2019, Militz 2020, Sangregorio *et al*. 2020).

In recent years, furfuryl alcohol (FA), which can be obtained through the hydrogenation of pentosans present in agricultural by-products, has been successfully implemented in wood chemical modification (Schneider 1995, Westin 1996, Westin *et al*. 1998, Lande *et al*. 2004, Nordstierna *et al*. 2008, Lande *et al*. 2008a, 2008b, Li *et al*. 2016, Mantanis 2017). Actually, the researchers M. Schneider (University of New Brunswick) and M. Westin (SP Sweden, RISE), separately, developed during the 90's, alternative catalysts for the furfurylation process, i.e. cyclic carboxylic anhydrides mainly maleic anhydride (Li *et al*. 2016, Mantanis 2017). An even more efficient process based on the vapour phase furfurylation of wood, is currently under development (Liu *et al*. 2020).

The furfurylation technology, which developed by Schneider and Westin, widely known today as *furfurylation*, is considered as an impregnation modification process, since it is believed that furfuryl alcohol is not chemically bound to the polymeric constituents of wood (Hill 2006, Rowell 2012). However, Lande *et al*. (2004, 2008a) have conceived that there should be a grafting reaction between lignin and furfuryl alcohol. Other scientists postulate that furfurylation involves a chemical modification, since FA polymer reacts with itself and possibly reacts with lignin in the cell walls of wood (Gérardin 2016, Li *et al*. 2016).

CONTACT George I. Mantanis mantanis@uth.gr Department of Forestry, Wood Sciences and Design, Laboratory of Wood Science and Technology, University of Thessaly, Karditsa GR 43100, Greece; Roger Moya rmoya@itcr.ac.cr InstitutoTecnológico de Costa Rica, Escuela de Ingeniería Forestal, Apartado 159-7050, Cartago, Costa Rica

As a matter of fact, polymerisation of FA is a complex process (Thygesen *et al*. 2020). It requires a catalyst, and presently is considered to occur in three steps (Choura *et al*. 1996). Step I comprises the formation of linear FA chains, which in the second step (step II) form conjugated FA oligomers. Such steps take place while the system is still liquid. At the final, step III, the linear oligomers crosslink via *Diels–Alder* cycloadditions forming a branched structure. This bases the emergence of a rubbery state, a procedure that, if allowed to advance even further, results in a stiff and glassy, hard polymer. Whether or not FA links to lignin inside the cell walls of furfurylated wood, has been argued over the years (Mantanis 2017). Experiments *in vitro* have revealed that FA links to ring positions of simple lignin monomers (Nordstierna *et al*. 2008), while molecular modelling using larger, more realistic lignin models indicated that FA just as readily binds to other molecular positions, not present in the simpler lignin models (Barsberg and Thygesen 2017). The modelling study on lignin models by Barsberg and Thygesen (2017) concluded that bonding to the C-alfa can be the most possible bonding point in lignin, rather than positions on the rings. Significantly, it is now believed that bonding to –OH groups does not seem to happen based on thermodynamic considerations (Barsberg and Thygesen 2017, Thygesen *et al*. 2020).

Additionally, it was found that elongation of FA chains, that is, step II in the polymerisation process according to Choura *et al*. (1996), takes place readily in the lumina, and not so much inside the cell walls, presumably due to sterical hindrance (Thygesen *et al*. 2010). Also, possible differences in the curing products, and their distribution within the compound cell walls (Thygesen *et al*. 2010), clearly depend upon the anatomical features of each wood species (Bertarione *et al*. 2008). Most studies considering this type of wood modification have focused on the effect of FA on softwoods, mostly pines, by applying different catalysts (Venås and Rinnan 2008). In accordance with the three-step mechanism proposed by Choura *et al*. (1996), Thygesen *et al*. (2010) observed that furfurylation causes a strong fluorescence originating from the FA-derived conjugated polymer segments, located both within cell walls and within lumens, as exhibited by fluorescence spectroscopy and confocal laser scanning microscopy. The fluorescence characteristics were closely coupled with the location of the polymer. Markedly, the emission from cell lumen material was significantly red-shifted as compared to emission originating from within cell walls, thus proving that the propensity of the FA polymer to form longer conjugated segments is indeed much higher in the less constrained (empty) cell lumina.

In their comprehensive study, Barsberg and Thygesen (2017) proposed that furfurylated wood cell walls can be described as a poly(FA)-wood hybrid material, in which, poly(FA) is efficiently trapped by covalent bond formation to lignin, e.g. as a poly(FA)-lignin co-polymer. Besides, a pure FA polymer can be trapped in the cell wall by entanglement; i.e. covalent binding is thus not necessary. This co-polymer formation hinders leaching of poly(-FA) and forms a kinetic barrier for moisture access to wood hydroxyl groups.

Meanwhile, studies on the furfurylation of tropical species are limited, up to date (Hadi *et al*. 2020). Tropical hardwood species are characterised by a lignin percentage, type and distribution quite different than that of softwood species (Saka 2000, Simon *et al*. 2018). In tropical species, guaiacyl lignin is present mainly in the vessels, whereas, syringyl-guaiacyl lignin is located in the secondary walls of fibres and rays (Saka 2000). On the contrary, in softwoods, lignin is composed typically of the guaiacyl type (Zhou *et al*. 2016). The percentage and chemical type of lignin in hardwoods vary largely among species and genera (Saka 2000, Bose *et al*. 2009).

Further, intensive research is presently carried out on nanotechnology treatments, which are related to numerous areas, from materials science to medicine (Scott and Chen 2013). Wood, a lignocellulosic complex, is thus the substrate of several nanotechnology-based techniques, which seek out to improve its material properties and products thereof (Tarmian *et al*. 2012). Nevertheless, most of the studies have focused on the enhancement of its biological durability (Lykidis *et al*. 2013, Mantanis *et al*. 2014, Lykidis *et al*. 2016, Taghiyari *et al*. 2020a, 2020b). Several types of nanoparticles have gained popularity in an attempt to upgrade the wood material (Mie *et al*. 2013).

As a matter of fact, the use of FA along with different nanoparticles has been researched in the last decade, as reviewed by Taghiyari *et al*. (2020a). For example, Dong *et al*. (2014) fabricated wood/polymer nanocomposites between FA and nano-SiO2 into fast-growing poplar wood. They found that its dimensional stability, water uptake and surface hardness were significantly improved. Also, Gao *et al*. (2017) experimented on composites of FA and gel into nano-Al_2O3 with the objective to improve the thermal stability, dimensional stability and dynamic wettability. Rahman *et al*. (2018) studied nanocomposites composed of wood and nanoclay to upgrade the wood properties. Nevertheless, the application of silver nanoparticles in combination with FA is the least studied. For instance, in tropical juvenile wood, the incorporation of silver nanoparticles in the cell wall has shown to increase its resistance to biological decay, when silver nanoparticles were used at liquid concentrations of 50 ppm (Moya *et al*. 2014a, 2014b, 2017).

In Central America, Costa Rica is presently implemented reforestation programs by developing fast-growing plantations with a variety of species, focusing mostly for lumber production (Moya *et al*. 2015). In these programs, early-age tree harvesting yields mainly juvenile wood (Adebawo *et al*. 2016), which is characterised by low quality and durability (Adebawo *et al*. 2016, Moya *et al*. 2019). A variety of treatments has been experimented in order to advance the physical, mechanical and biological properties of the tropical woods (Moya *et al*. 2017, Moya *et al*. 2020a, 2020b, Gaitán-Alvarez *et al*. 2020). Therefore, this study focused on the modification of tropical hardwood species with furfuryl alcohol (FA) alone, and FA in combination with silver nanocompounds (FA-NPsAg), and subsequent analyses of treated materials with the use of confocal laser scanning microscopy (CLSM) and Fourier-transform infrared spectroscopy (FTIR).

Materials and methods

Materials

Sapwood samples from nine fast-growing species, from plantations in Costa Rica, were used in the work. Such materials have sufficient permeability and satisfactory behaviour in wood modification experiments (Moya *et al*. 2017, 2020a, 2020b, Gaitán-Alvarez *et al*. 2020). Tropical wood species used in the work included: i) species with very low specific gravity (≤0.35 g/cm^3), namely, Spanish cedar *(Cedrela odorata)*, chanco blanco *(Vochysia guatemalensis)* and guanacaste *(Enterolobium cyclocarpum)*, and (ii) species with medium specific gravity (0.35–0.56 g/cm^3), such as Spanish elm *(Cordia alliodora)*, gmelina (*Gmelina arborea)*, pilón *(Hieronyma alchorneoides)*, rain tree *(Samanea saman)*, teak *(Tectona grandis)*, and chancho colorado *(Vochysia ferruginea)*. Detailed description of these species can be found elsewhere (Moya *et al*. 2020a, 2020b). The materials originated from forest plantations varying from 4- to 8-year old trees, using three different trees from each species. Once sawn and kiln-dried, planks were climatised to a moisture content of approximately 12%, and afterwards, forty-five, free-defects specimens measuring 50 mm x 50 mm x 20 mm (tangential x radial x longitudinal) were prepared for every species.

The chemical reagents used in this work were: furfuryl alcohol at 98% solution (Sigma Aldrich, Belgium), sodium borate 10-hydrate (J.T. Baker, Madrid), citric acid (Central Drug House, New Delhi), and oxalic acid dehydrate (Oxford Lab Fine Chem, Maharastra, India). Three components were employed for the synthesis of silver nanoparticles (NPsAg), namely, silver nitrate ($AgNO_3$) as a source of reduced metal (MERCK; pureness 99.9%), ethylene glycol ($C_2H_6O_2$) as a reducing agent (J.T. Baker; pureness 99.9%), and polyvinyl pyrrolidone as a stabilising agent (Magnacol Ltd., UK). The synthesis procedure used has been described in previous studies (Moya *et al*. 2014a, 2017).

Treatments

Two treatments were employed for the furfurylation of wood samples: (i) a treatment, labelled as FA (Rowell 2012, Sandberg *et al*. 2017), which included a furfuryl alcohol solution, composed of FA (50%), distilled water (46.2%), sodium borate as buffer agent (2%) and organic acid as a catalyst, composed of oxalic acid and citric acid (1.75% in total), and (ii) a second treatment, labelled as FA-NPsAg, which comprised of the same constituents, as the first treatment, also incorporating a 50 ppm proportion of silver nanoparticles. This proportion was incorporated in accordance with the study of Moya *et al*. (2017).

Furfurylation process in the laboratory

Furfurylation trials were carried out in the laboratory according to typical methods for furfurylation process (Mantanis 2017), in which wood samples were located in a vacuum-pressure reactor, in our studied of 2.5 l in capacity. Fifteen wood samples were introduced in the reactor for vacuum application for 45 min, in absolute vacuum (approx. -30 kPa), and then, either FA or FA-NPsAg was introduced in the reactor. Afterwards, a 690 kPa pressure was applied for 2 h, after which, the excess of liquid solution was emptied from the reactor, and the samples were cleaned to remove the excess solution from their surfaces. Inside temperature in the reactor was fixed at 40°C for 4 h, applying, again, absolute vacuum for 20 min. Following the 4 h time, the samples were extracted from the reactor and wrapped in aluminium foil, thus, avoiding the drying of wood. Then, they were placed in a laboratory drier for 16 h at 103°C in order to induce the reaction. After this period, samples were left for another 24 h at 103°C in order to reach the oven-dried state (0% moisture condition).

Evaluation of weight percentage gain (WPG)

For each furfurylation treatment used (FA; FA-NPsAg), fifteen samples were measured, and another fifteen samples were left untreated ('control group') for comparative purposes. Samples were placed into the oven for 24 h, before and after each furfurylation treatment, and their weight and dimensions were measured. Weight percentage gain of wood was calculated according to Equation (1), considering the weight of the sample in oven-dry condition, as the initial weight.

$$\text{Weight percentage gain } (WPG) = \frac{\text{Weight}_{\text{after furfurylation}}(g) - \text{Weight}_{\text{before furfurylation}}(g)}{\text{Weight}_{\text{before furfurylation}}(g)} \quad (1)$$

Confocal laser scanning microscopy (CLSM)

From each species, two samples per each treatment, from the centre of the piece, were selected to obtain 15 µm thickness microtome cuts using an American Optical Corp model 860 microtome to achieve smooth surfaces. These samples were not dyed so as to observe a clearer fluorescence. The analytical instrument used was a confocal laser scanning microscope (model TCS SP2, Leica Microsystems, Germany) with a 639 objective (water immersion). The excitation laser wavelengths applied were 600 nm, while the detector ranges were 500–550 and 550–600 nm according to Thygesen *et al*. (2020). We decided to use this wavelength (600 nm), because this excite the longer chains in the FA polymer, present in the lumina. The same gain setting was used, thus allowing direct comparison of emission intensities for images obtained using the same excitation wavelength. In order to reduce noise, images were recorded as averages of eight frames. The images were stored as 1024 × 1024 pixels in tiff files. The images were colour-coded according to emission intensity, with colour going from black over red and yellow to white, while blue indicates detector overload (Thygesen *et al*. 2010). Two images were obtained per each species, one of a treated sample and one of an untreated sample.

Fourier-transform infrared (FTIR) spectroscopy

Three samples, randomly selected per each treatment, were taken from each wood species, i.e. 3 for FA, 3 for FA-NPsAg and 3 for untreated samples. Each sample was ground to 420 and 250 µm sizes, respectively (40 mesh and 60 mesh, respectively). Samples were kiln dried at 105°C until reaching a constant weight. The FTIR spectra for the samples were acquired using a Thermo Scientific Nicolet 6700 (Thermo Scientific, IL, USA), equipped with an attenuated total reflectance accessory within a range of 3800–800 cm^{-1}, a resolution of 4 cm^{-1}, and 16 scans. The FTIR spectra obtained were processed with the Spotlight 1.5.1, HyperView 3.2 and Spectrum 6.2.0 software, developed by Perkin Elmer (Massachusetts, USA). Of the three selected samples per treatment, only a single one was selected to be represented as the best fit in. The vibrations, where the spectra from the furfurylated wood differed markedly from the spectra of the corresponding untreated wood, were well identified (Dong *et al*. 2014, Gao *et al*. 2017, Kong *et al*. 2018). The FTIR spectrum was transformed to transmission spectra and the ATR correction was applied. For the FA treatment, the changes were located in the bands at 773 cm^{-1} (furan rings of FA), 796 cm^{-1} (C=O stretch of γ-diketones), 889 cm^{-1} (carbonyl stretching and β-glucosidic linkages between the sugar units), 1561 cm^{-1} (C=O stretching vibration of the γ-diketone), 1652 cm^{-1} (carbonyl stretching), and 1711 cm^{-1} (C=O stretching vibration). For the FA-NPsAg treatment, the peaks were identified at 1016 cm^{-1} (C–O stretch), 1224 cm^{-1} (CO and OH groups), 1370 cm^{-1} (C–H vibration in cellulose), 1426 cm^{-1} (C–H in plane deformations and C–H deformation in lignin and carbohydrates), and 1505 cm^{-1} (aromatic skeletal vibrations in lignin), all above, according to previous studies of Xie *et al*. (2013) and Can *et al*. (2018, 2019).

Statistical analysis

Tests for normality, homogeneity of data, and also, elimination of atypical data (or outliers) were carried out regarding the WPG values per individual specimen. Afterwards, a descriptive analysis was made with determination of the mean standard deviation and coefficient of variation. A variance ANOVA analysis, with a statistical significance value of $p<0.05$, was applied to determine the effects of each furfurylation treatment (independent variable) on the WPG. The mixed linear model was used in the analysis of variance of wood properties (Equation 2). Tukey's test was used to determine the statistical significance of the differences between the means of the variables. In addition, statistical analysis was performed with the use of SAS 9.4 software (SAS Institute Inc., USA).

$$Y_i = \mu + \tau_i + \varepsilon_i \quad (2)$$

where Y_i is the single observation of WPG of the i_{th}-observation, µ is the overall mean, τ is the ith-furfurylation random effect, and ε_i is the residual random effect.

Results and discussion

Weight percentage gain

Weight percentage gain of wood tested in this work, varied from 44.2% to 14.4% with the FA treatment, and from 44.5% to 12.9% with the FA-NPsAg treatment (Figure 1(a, b)). According to a recent review (Mantanis 2017) and analysis study by Li *et al*. (2015) carried out in several softwood species, typical WPG values commonly varied from 15% to 100%. The WPG values obtained in this work varied from 14.4% to 44.5%, that is, they are in this value range as reported in the bibliography (Li *et al*. 2015, Mantanis 2017).

In general, WPG was affected by species, furfurylation treatment and their interaction (Table 1). Thus, the difference was the highest WPGs for FA treated wood appeared in the species *V. guatemalensis* and *V. ferruginea*, while the lowest WPGs were observed in *Cedrela odorata*, *Gmelina arborea* and *Tectona grandis* (Figure 1(a)). In FA-NPsAg treated wood, the highest WPG values were occurred also in *V. guatemalensis* and *V. ferruginea*. However, statistically different values were shown for the species *C. odorata*, *S. saman*, *E. cyclocarpum* and *T. grandis* (Figure 1(b)). Regarding differences in each species, it was found that WPG was statistically lower in *S. saman* and *E. cyclocarpum* wood, when treated with FA-NPsAg. The other wood species did not show this particular statistical difference (Figure 1(c)). In the FA-NPsAg treatment for *S. saman* and *E. cyclocarpum* species, it was observed that the solution of FA-NPsAg incremented the viscosity in the moment that the solution came in contact with wood; afterwards, the absorption decreased. The solution of NPsAg was unstable (Moya *et al*. 2014a, 2014b, 2017), that is to say, the chemical composition of *S. saman* and *E. cyclocarpum* woods possibly influenced the stability of the FA-NPsAg solution.

WPG values, in this work, showed a large variation, a typical characteristics for tropical hardwood species subjected to treatments involving the permeability of wood (Ahmed and Chun 2009). The same variation, in the retention of chemicals, has been observed in the same tropical species for treatments such as preservation (Moya *et al*. 2019), mineralisation (Moya *et al*. 2020a, 2020b), and acetylation (Gaitán-Alvarez *et al*. 2020). It is well known that liquid absorption in wood is related to the permeability of the species, which mostly varies as a function of the anatomical elements of the species itself (Ahmed and Chun 2009) and other properties such as wood density (Tarmian *et al*. 2020). Similarly for furfurylation, permeability of the cellular walls is of utmost importance (Thygesen *et al*. 2010, Li *et al*. 2016). In hardwood species, liquid flow occurs chiefly along the lumina vessels in the longitudinal direction (Ahmed and Chun 2009, Tarmian *et al*. 2020). Vessels are connected with the longitudinal and radial parenchyma across the wall pits, so liquids can flow through the radial lumina (Tarmian *et al*. 2020). Variations in the anatomical features of wood species, as in a previous study on acetylation, are presented in Table 1 of studied Gaitán-Álvarez *et al*. (2020a). In fact,

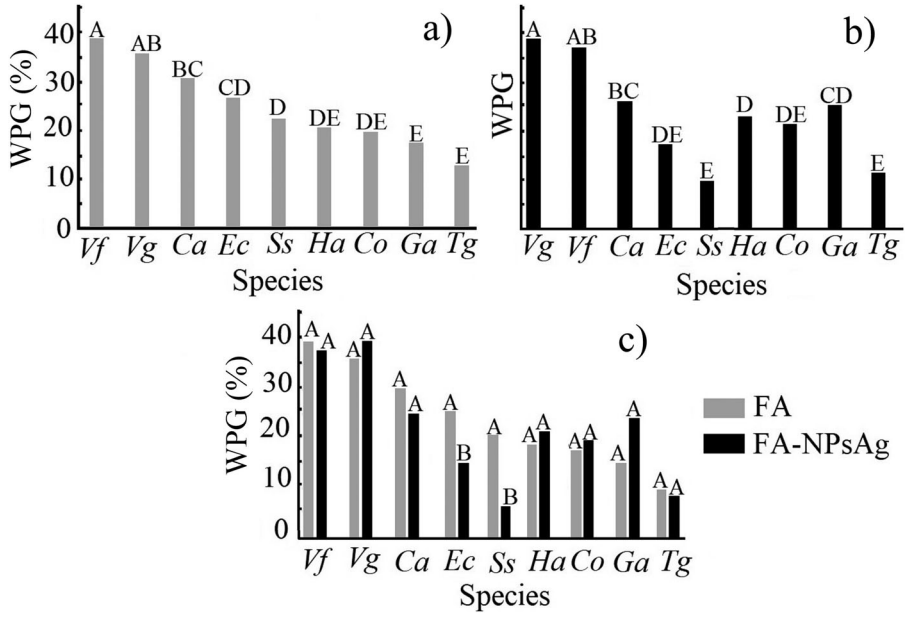

Figure 1. WPGs of tropical hardwood species treated with furfuryl alcohol (a), and furfuryl alcohol with silver nanoparticles (b). Comparison of WPGs between the two treatments (c). Note 1: a, b: Different characters between species indicate statistical differences at 95%. c: Different characters between treatments FA and FA-NPsAg indicate statistical differences at 95%. Note 2: *Cedrela odorata (Co); Cordia alliodora (Ca); Enterolobium cyclocarpum (Ec); Gmelina arborea (Ga); Hieronyma alchorneoides (Ha); Samanea saman (Ss); Tectona grandis (Tg); Vochysia ferruginea (Vf); Vochysia guatemalensis (Vg)*. The species are listed from the highest WPG to the lowest WPG.

Gaitán-Álvarez *et al.* (2020a) reported that species like *E. cyclocarpum*, *H. alchorneoides*, *S. saman*, *V. ferruginea* and *V. guatemalensis* are characterised by anatomical features of much larger dimensions, that is: diameter of vessels over 120 µm, width of rays from 2 to 10 series of cells, or over 252 µm, and ray frequency over 5 rays/mm^2, as well as several types of axial parenchyma (Gaitán-Álvarez *et al.* 2020a). Such anatomical characteristics favour the flow of solutions, which is in accordance with the findings of the present study, since the above-mentioned species presented, undeniably, the highest WPG values. On the contrary, the species which exhibited the lowest WPGs (*C. odorata*, *G. arborea*, *T. grandis*) possess anatomical elements less favourable for liquid flow, like smaller and less frequent rays, and many deposits in the vessels, such as gums and tyloses (Gaitán-Álvarez *et al.* 2020a).

An aspect to highlight, from the outcome of the present work, is that such forest-plantation wood materials typically have low percentage, or no heartwood (Moya *et al.* 2019), unlike the wood originating from mature trees of natural forests, in which, a high heartwood portion is commonly present (Moya *et al.* 2009). Therefore, it is expected that such wood material, from natural forest trees, will result in much lower WPGs due to the very poor permeability of the heartwood itself (Ahmed and Chun 2009).

Table 1. Results of ANOVA analysis showing the effects of wood species and furfurylation treatment on the WPG.

Variation source	Degree freedom	Mean square	*F*-value
Type of species (A)	8	3961.98	37.30**
Furfurylation treatment (B)	1	191.71	1.81**
A x B	8	526.27	4.96**
Error	327	106.21	–
Total	244	–	

**Statistically significant at 99% confidence level; *statistically significant at 95% confidence level; ns: not significantly different.

Analysis with CLSM

By means of fluorescence, the CLSM observations of tropical wood species used (both treated and untreated) revealed a high variability per species and per FA treatment used, in respect to the degree of penetration into the different areas of wood anatomical elements (Thygesen *et al*. 2010, Donaldson 2013). This directly influenced the overall degree of furfurylation itself. Untreated material of species like *E. cyclocarpum*, *G. arborea* and *H. alchormoides* presented autofluorescence at 600 nm (Figure 2(d1, f1, h1)), in contrast to untreated wood from the other species, which did not present this autofluorescence (Figure 2(a1, b1, c1, e1, g1, i1)). In respect to fluorescence at 600 nm, minimal difference was observed between the FA and FA-NPsAg treatment for a given species, with the noticeable exception of species *S. saman*, in which, the FA-NPsAg treatment presented a higher fluorescence as compared with that with the FA treatment (Figure 2(e2, e3)).

The degree of furfurylation varied among regions close to the different anatomical elements. Moreover, some differences appeared between the two FA treatments and among the different tropical species. In most of the species, the cell walls of the fibres were largely furfurylated (Figure 3); however, rays showed a low intensity indicating a smaller degree of furfurylation in the close by region (Figure 3(a–f)). Fluorescence intensity was 'affected' by the type of parenchyma, for a given wood species. For example, species like *C. odorata*, *G. arborea* and *Tectona grandis*, that have scanty paratracheal parenchyma, or vasicentric

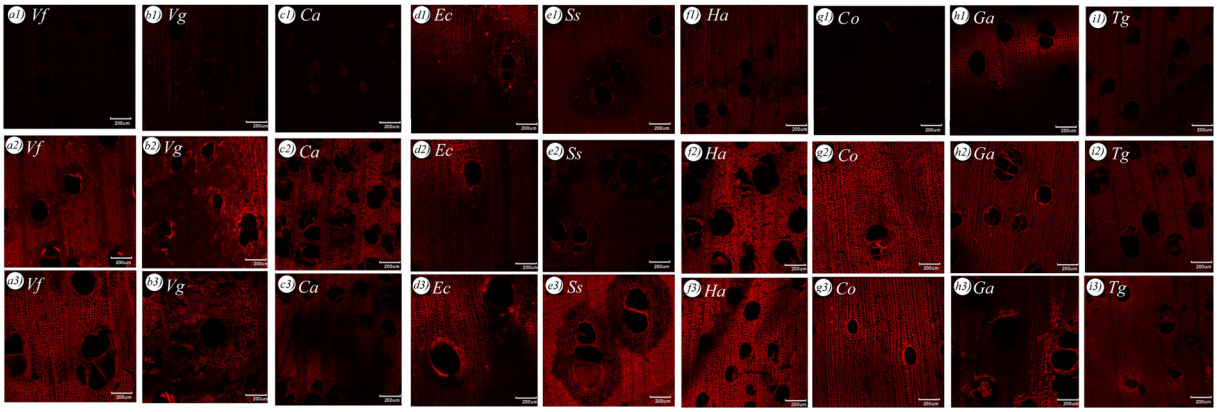

Figure 2. Fluorescence through confocal laser scanning microscopy indicating the high FA absorption in different areas of wood anatomical features. Note: *Cedrela odorata (Co); Cordia alliodora (Ca); Enterolobium cyclocarpum (Ec); Gmelina arborea (Ga); Hieronyma alchorneoides (Ha); Samanea saman (Ss); Tectona grandis (Tg); Vochysia ferruginea (Vf); Vochysia guatemalensis (Vg).* The species are listed from the highest WPG to the lowest WPG.

parenchyma, showed around the vessels a low intensity of fluorescence (Figure 3(c,d)). In species *E. cyclocarpum*, the low intensity fluorescence was particularly observed around the vessels and the lozenge-aliform parenchyma (Figure 3 (b)). Where axial, winged-aliform or confluent parenchyma was present, a low intensity fluorescence was displayed as well (Figure 3(a)). Markedly, results of fluorescence at 600 nm pointed out that some wood species presented a high intensity around the vessels (Figure 3(a, b, d)), as well as in the middle lamella between two vessels (Figure 3(a, e)).

In tropical species, fibres are the elements constituting of the greater amount of lignin (Higuchi 1997), specifically, mostly of syringyl and guaiacyl lignin (Saka 2000, Simon *et al*. 2018). With the optimum amount of FA, cell walls of fibres showed high fluorescence, especially in the species *V. ferruginea*, *V. guatemalensis* and *C. alliodora* with high WPGs (Figure 2(a–c)). In addition, the lower content of lignin in parenchyma (radial or axial), compared to fibres and vessels (Saka 2000, Donaldson 2013), showed the scarce lignification in the ray walls (Figure 2(d, e, g, i)), or in

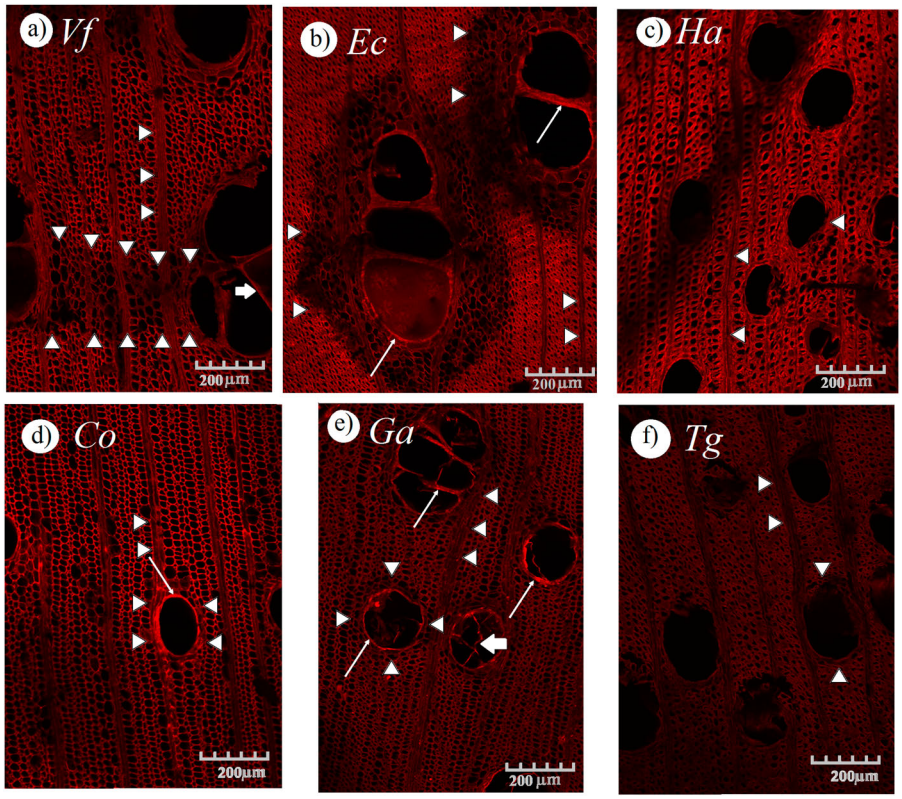

Figure 3. Fluorescence at CLSM in the different areas of anatomical features of *Vf*: *Vochysia ferruginea* (a), *Ec*: *Enterolobium cyclocarpum* (b), *Ha*: *Hieronyma alchorneoides* (c), *Co*: *Cedrela odorata* (d), *Ga*: *Gmelina arborea* (e), and *Tg*: *Tectona grandis* (f) wood. Note: ∇ indicates low intensity fluorescence in rays or paratracheal parenchyma; → high intensity fluorescence around the vessels; ⇨ fluorescence in the middle lamella.

the scanty paratracheal parenchyma (Figure 3(d)), lozenge-aliform or winged-aliform, or vasicentric parenchyma (Figure 3(b)). Also, in confluent parenchyma (Figure 3(d)), which was present in few of the species studied. The lignin concentration in the cell wall of vessels, as well as higher degree present in the middle lamella between vessels (Simon *et al*. 2018, Donaldson 2020) are quite evident in the species *C. odorata*, *E. cyclocarpum* and *G. arborea* (Figure 3(b, d, e)).

Analysis with FTIR spectroscopy

The wavenumbers of FTIR spectrum, ranging from 650 to 4000 cm^{-1}, revealed the response of the organic portions of wood from 650 up to 1800 cm^{-1}; this range corresponded to cellulose, hemicelluloses and lignin (Berrocal *et al*. 2016). This region of the spectrum was present for all the species (Figure 4). Regarding the inorganic portions, previous studies indicated that, for some NPsAg additions, an increment of vibrations appeared at 3422 cm^{-1} corresponding to O–H bond stretching vibrations, and another increment was present at 2910 and 2840 cm^{-1} corresponding to asymmetric and symmetric stretching vibrations for C-H bonds, respectively (Can *et al*. 2018, 2019). In this study, in wood treated with FA-NPsAg, no increase in intensity was observed in the 3422, 2840 and 2910 cm^{-1} regions. Probably, the concentration of NPsAg was not sufficient enough to induce any changes in these bonds' behaviour; e.g. the present work used a 50 ppm addition, whereas, Can *et al*. (2018, 2019) applied much higher NPsAg concentrations (between 0.4% and 1.5%).

Nevertheless, other researchers have indicated that in the FTIR spectra of the organic portion of furfurylated wood, changes occurred in bands of 1711, 1652, 1561, 889, 796 and 733 cm^{-1} (Dong *et al*. 2014, Gao *et al*. 2017, Kong *et al*. 2018). On the other hand, in wood treated with NPsAg, changes took place in bands of 1711, 1505, 1426, 1370, 1224 and 1016 cm^{-1} (Johnston and Nilsson 2012, Xie *et al*. 2013, Can *et al*. 2019).

Respecting the previous studies, the vibration in 1711 cm^{-1} wavenumber showed an increase for all wood species, as compared to untreated wood, but simultaneously, no differences were observed between the FA treated and FA-NPsAg treated wood material (Figure 4). According to Can *et al*. (2018, 2019), the increase in vibration is another indicator of the NPsAg presence. In this work, when wood was furfurylated only with FA, the vibration increases attributed to C=O bond stretching vibration of the γ-diketone formed from hydrolytic ring opening of the furan of FA, whereas, in wood treated with NPsAg, the vibration increase owed to the alteration of an unconjugated C=O stretch of the acetyl and carbonyl group of xylans in hemicelluloses. Therefore, we consider that FA affected the hydrolytic ring of the furan as well as the acetyl and carbonyl groups of the xylans in hemicelluloses.

Vibration at 1652 cm^{-1}, assigned to the conjugated carbonyl stretching (Dong *et al*. 2014), presented no differences between both FA treatments, nor with the untreated wood (Figure 4). Consequently, no lignin hydrolysis has taken place, as the change in vibration at 1652 cm^{-1} can be attributed to this modification (Dong *et al*. 2014). In regard to the vibration at 1561 cm^{-1}, corresponding to skeletal vibrations of 2,5-disubstituted furan rings (Ahmad *et al*. 2013), a difference appeared between the two treatments used, but this effect varied from one species to another (Figure 4). Specifically, wood from *V. ferruginea*, *V. guatemalensis*, *C. odorata*, *S. saman* and *E. cyclocarpum* (i.e. species with WPGs >25%) exhibited higher vibration intensities with the FA treatment, than that of the FA-NPsAg treatment (Figure 4(a–e)). Conversely, species with WPG lower than 20% (*C. alliodora*, *G. arborea*, *H. alchornoides*, *Tectona grandis*) showed similar intensities between the FA and FA-NPsAg treatment (Figure 4(f–i)). This outcome clearly indicates that wood species (with higher furfurylation effects, i.e. WPG >25%) undergo a higher degree of modification of the furan rings, thus suggesting a much higher modification of the lignin structures, in wood species with higher WPG values.

For vibrations at 889 cm^{-1}, attributed to β-glucosidic linkages between sugar units (Kong *et al*. 2018), an intensity increase was observed in the wood species which showed a WPG >25% with the FA treatment, namely *V. ferruginea*, *V. guatemalensis*, *C. odorata*, *S. saman* and *E. cyclocarpum* (Figure 4(a–e)). The rest of the species presented a quite similar intensity between the FA and FA-NPsAg treatment (Figure 4(f–i)). For all species tested, the intensity of vibrations decreased with both of the treatments (Figure 4). Subsequently, these results suggest that the hemicelluloses underwent a modification by acid hydrolysis (Kong *et al*. 2018), most noticeably, in the species with higher WPG values.

wFor vibration intensities at 796 and 733 cm^{-1}, attributed to skeletal vibrations of 2,5-disubstituted furan rings (Oishi *et al*. 2012, Yang *et al*. 2019), wood species like *V. ferruginea*, *V. guatemalensis*, *C. odorata*, *E. cyclocarpum*, *C. alliodora*, *H. alchornoides* and *Tectona grandis* furfurylated with FA and FA-NPsAg exhibited much higher vibrations than that of untreated wood (Figure 4(a–c, e, f, h–i)). In *S. manan*, the highest vibration intensity showed with the FA treatment, though, FA-NPsAg treated and untreated wood were not different from each other (Figure 4(d)). Also, for *Gmelina arborea*, the vibration intensity was higher with the FA-NPsAg treatment, while with FA treated gmelina wood and untreated one presented not different vibrations (Figure 4(g)). Hence, these results indicated that there was a vibration in the furan ring, which was formed during furfurylation of wood, mainly in species with a higher WPG value.

Vibrations at intensities of 1711, 1505, 1426, 1370, 1224 and 1016 cm^{-1} corresponded to the presence of NPsAg (Xie *et al*. 2013, Can *et al*. 2018, 2019). As Johnston and Nilsson (2012) previously indicated, the increase at 1711cm^{-1} can be erroneous for the vibration increase from the FA treatment. For the remaining vibrations (Figure 4), a higher intensity of the vibrations was observed at 1505 cm^{-1} and 1016 cm^{-1} for all wood species modified with the NPsAg treatment (Figure 4). Xie *et al*. (2013) suggested that the higher vibration intensity at 1505 cm^{-1} can be attributed to a modification in the aromatic band of lignin's syringyl rings by the presence of

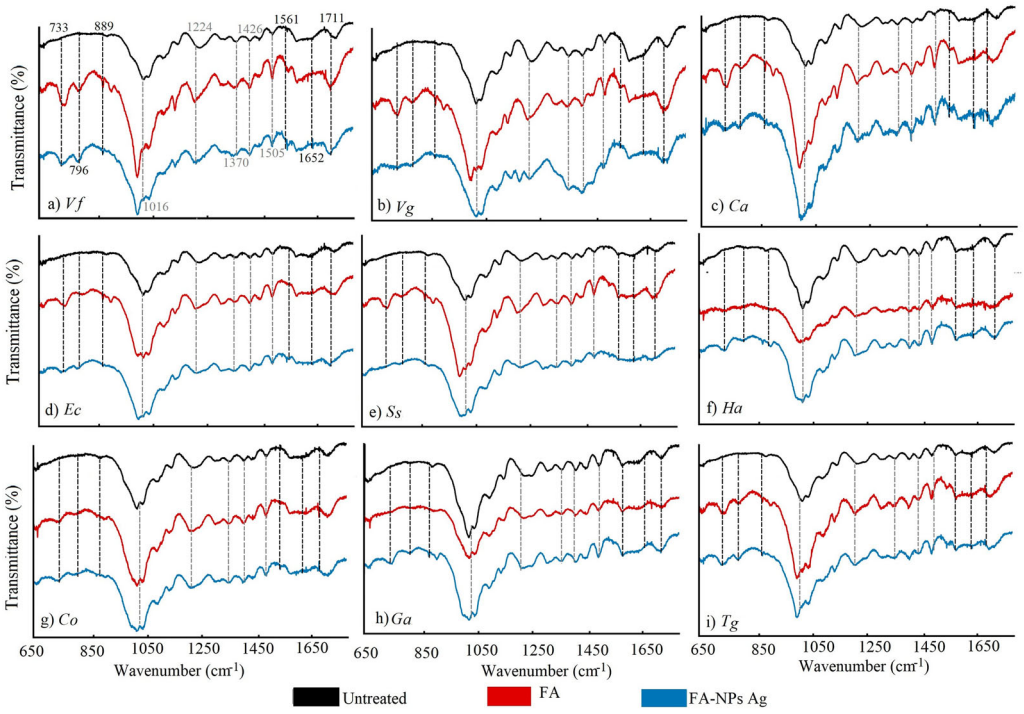

Figure 4. FTIR spectra from 650 to 1800 cm^{-1} of tropical wood materials modified with the two different furfurylation treatments. Note: *Cedrela odorata (Co); Cordia alliodora (Ca); Enterolobium cyclocarpum (Ec); Gmelina arborea (Ga); Hieronyma alchorneoides (Ha); Samanea saman (Ss); Tectona grandis (Tg); Vochysia ferruginea (Vf); Vochysia guatemalensis (Vg)*. The species are listed from the highest WPG to the lowest WPG.

silver nanoparticles. The band at 1016 cm^{-1}, owing to the C-O bond stretch manifested in cellulose and hemicelluloses, clearly evidenced changes in this bond by an increase in vibration, due to the presence of FA-NPsAg. Unexpectedly, no difference was observed between the various wood species, probably because the NPsAg concentration was rather insufficient for a noticeable change to occur in the bonds. In previous works, as noted earlier, that concentration was higher at 0.4% (Can *et al*. 2018, 2019), whereas, in this study, a much lower concentration (50 ppm) was applied.

Conclusions

Furfurylation of tropical species, originating from Costa Rican forest plantations, with and without the addition of silver nanoparticles, was carried out in the laboratory. In general, WPG of wood varied from 44.3% to 14.4% with the plain FA treatment, and from 44.5% to 12.9% for the FA-NPsAg treatment. On the whole, no statistical differences (p-values>0.05) were observed between the FA treatment and the FA-NPsAg treatment used.

The highest WPG values (e.g. WPGs>30%) with the FA treatment, were exhibited with the species *V. guatemalensis* and *V. ferruginea*, while the lowest ones (WPGs< 30%) were observed in *Cedrela odorata*, *Gmelina arborea* and *Tectona grandis* species. As expected, the flow of solutions was favoured in wood species having the suitable anatomical features, specifically, diameter of vessels over 120 μm, width of rays from 2 to 10 series of cells, or over 252 μm, and ray frequency over 5 rays/mm^2 as well as several types of axial parenchyma.

The degree of furfurylation achieved diverged among the different areas of anatomical elements; that is, in most of the species, cell walls of fibres were highly furfurylated, while the areas around the rays, or paratracheal parenchyma, showed low intensity indicating a much lower degree of furfurylation in the region, possibly due to the low lignin content.

Future work should focus on the evaluation of the physical and moisture properties as well as the decay resistance of furfurylated tropical woods treated in here, so as to assess the efficiency of the aforementioned treatments.

Acknowledgements

The authors thank Vicerrectoría de Investigación y Extensión of Instituto Tecnológico de Costa Rica (ITCR, Cartago, Costa Rica) for the financial support provided. The research project was carried out in close collaboration with the Laboratory of Wood Science and Technology, University of Thessaly (Dept. of Forestry, Wood Sciences and Design). Professor G. Mantanis acknowledges the contribution of program *Erasmus+ KA107* (International Credit Mobility) for enabling this type of research cooperation between ITCR (Costa Rica) and University of Thessaly (Greece).

Disclosure statement

No potential conflict of interest was reported by the author(s).

Funding

The authors thank Vicerrectoría de Investigación y Extensión of Instituto Tecnológico de Costa Rica (ITCR, Cartago, Costa Rica) for the financial support provided.

References

Adebawo, F. G., Naithani, V., Sadeghifar, H., Tilotta, D., Lucia, L. A., Jameel, H. and Ogunsanwo, O. Y. (2016) Morphological and interfacial properties of chemically-modified tropical hardwood. *RSC Advances*, 6(8), 6571–6576.

Ahmad, E. E. M., Luyt, A. S. and Djoković, V. (2013) Thermal and dynamic mechanical properties of bio-based poly(furfuryl alcohol)/sisal whiskers nanocomposites. *Polymer Bulletin*, 70(4), 1265–1276.

Ahmed, S. A. and Chun, S. K. (2009) Observation of liquid permeability related to anatomical characteristics in *Samanea saman*. *Turkish Journal of Agriculture and Forestry*, 33(2), 155–163.

Barsberg, S. T. and Thygesen, L. G. (2017) A combined theoretical and FT-IR spectroscopy study of a hybrid poly(furfuryl alcohol) – lignin material: Basic chemistry of a sustainable wood protection method. *Chemistry Select*, 2, 10818–10827.

Berrocal, A., Moya, R., Rodriguez-Solis, M., Starbird, R. and Muñoz, F. (2016) Surface chemical and color characterization of juvenile *Tectona grandis* wood subjected to steam-drying treatments. *Surface Review and Letters*, 23(1). doi:10.1142/S0218625X15500912.

Bertarione, S., Bonino, F., Cesano, F., Damin, A., Scarano, D. and Zecchina, A. (2008) Furfuryl alcohol polymerization in H−Y confined spaces: reaction mechanism and structure of carbocationic intermediates. *The Journal of Physical Chemistry B*, 112(9), 2580–2589.

Bose, S. K., Francis, R. C., Govender, M., Bush, T. and Spark, A. (2009) Lignin content versus syringyl to guaiacyl ratio amongst poplars. *Bioresource Technology*, 100(4), 1628–1633.

Can, A., Palanti, S., Sivrikaya, H., Hazer, B. and Stefani, F. (2019) Physical, biological and chemical characterisation of wood treated with silver nanoparticles. *Cellulose*, 26(8), 5075–5084.

Can, A., Sivrikaya, H. and Hazer, B. (2018) Fungal inhibition and chemical characterization of wood treated with novel polystyrene-soybean oil copolymer containing silver nanoparticles. *International Biodeterioration & Biodegradation*, 133, 210–215.

Choura, M., Belgacem, N. M. and Gandini, A. (1996) Acid-catalyzed polycondensation of furfuryl alcohol: Mechanisms of chromophore formation and cross-linking. *Macromolecules*, 29, 3839–3850.

Donaldson, L. (2013) Softwood and hardwood lignin fluorescence spectra of wood cell walls in different mounting media. *IAWA Journal*, 34(1), 3–19.

Donaldson, L. (2020) Autofluorescence in plants. *Molecules*, 25(10), 2393.

Dong, Y., Yan, Y., Zhang, S. and Li, J. (2014) Wood/polymer nanocomposites prepared by impregnation with furfuryl alcohol and nano-SiO_2. *BioResources*, 9(4), 6028–6040.

Esteves, B., Nunes, L. and Pereira, H. (2011) Properties of furfurylated wood (*Pinus pinaster*). *European Journal of Wood and Wood Products*, 69(4), 521–525.

Gaitán-Alvarez, J., Berrocal, A., Mantanis, G. I., Moya, R. and Araya, F. (2020) Acetylation of tropical hardwood species from forest plantations in Costa Rica: an FTIR spectroscopic analysis. *Journal of Wood Science*, 66(1), 49.

Gao, X., Dong, Y., Wang, K., Chen, Z., Yan, Y., Li, J. and Zhang, S. (2017) Improving dimensional and thermal stability of poplar wood via aluminum-based sol-gel and furfurylation combination treatment. *BioResources*, 12(2), 3277–3288.

Gérardin, P. (2016) New alternatives for wood preservation based on thermal and chemical modification of wood – a review. *Annals of Forest Science*, 73(3), 559–570.

Hadi, Y. S., Herliyana, E. N., Mulyosari, D., Abdillah, I. B., Pari, R. and Hiziroglu, S. (2020) Termite resistance of furfuryl alcohol and imidacloprid treated fast-growing tropical wood species as function of field test. *Applied Sciences*, 10(17), 6101.

Higuchi, T. (1997) *Biosynthesis of Wood Components* (Berlin: Springer), 93, pp. 262.

Hill, C. A. S. (2006) *Wood Modification – Chemical, Thermal and Other Processes*, Wiley Series in Renewable Resources, Ed (Chichester: J. Wiley and Sons), pp. 260.

Johnston, J. H. and Nilsson, T. (2012) Nanogold and nanosilver composites with lignin-containing cellulose fibres. *Journal of Materials Science*, 47(3), 1103–1112.

Kong, L., Guan, H. and Wang, X. (2018) In situ polymerization of furfuryl alcohol with ammonium dihydrogen phosphate in poplar wood for improved dimensional stability and flame retardancy. *ACS Sustainable Chemistry & Engineering*, 6(3), 3349–3357.

Lande, S., Eikenes, M., Westin, M. and Schneider, M. H. (2008b) Furfurylation of wood: Chemistry, properties, and commercialization. *ACS Symposium Series*, 982, 337–355.

Lande, S., Westin, M. and Schneider, M. (2004) Properties of furfurylated wood. *Scandinavian Journal of Forest Research*, 19(5), 22–30.

Lande, S., Westin, M. and Schneider, M. (2008a) Development of modified wood products based on furan chemistry. *Molecular Crystals and Liquid Crystals*, 484(1), 367–378.

Li, W., Ren, D., Zhang, X., Wang, H. and Yu, Y. (2016) The furfurylation of wood: A nanomechanical study of modified wood cells. *BioResources*, 11(2), 3614–3625.

Li, W., Wang, H., Ren, D., Yu, Y. and Yu, Y. (2015) Wood modification with furfuryl alcohol catalysed by a new composite acidic catalyst. *Wood Science and Technology*, 49(4), 845–856.

Liu, M., Guo, F., Wang, H., Ren, W., Cao, M. and Yu, Y. (2020) Highly stable wood material with low resin consumption via vapor phase furfurylation in cell walls. *ACS Sustainable Chemistry & Engineering*, 8, 13924–13933.

Lykidis, C., Bak, M., Mantanis, G. and Németh, R. (2016) Biological resistance of pine wood treated with nano-sized zinc oxide and zinc borate against brown-rot fungi. *European Journal of Wood and Wood Products*, 74(6), 909–911.

Lykidis, C., Mantanis, G., Adamopoulos, S., Kalafata, K. and Arabatzis, I. (2013) Effects of nano-sized zinc oxide and zinc borate impregnation on brown-rot resistance of black pine (*Pinus nigra* L.) wood. *Wood Material Science and Engineering*, 8(4), 242–244.

Mantanis, G. I. (2017) Chemical modification of wood by acetylation or furfurylation: A review of the present scaled-up technologies. *BioResources*, 12(2), 4478–4489.

Mantanis, G., Terzi, E., Kartal, S. N. and Papadopoulos, A. (2014) Evaluation of mold, decay and termite resistance of pine wood treated with zinc- and copper- based nanocompounds. *International Biodeterioration and Biodegradation*, 90, 140–144.

Mie, R., Samsudin, M. W. and Din, L. B. (2013) A review on biosynthesis of nanoparticles using plant extract: An emerging green nanotechnology. *Advanced Materials Research*, 667, 251–254.

Militz, H. (2020) Wood modification research in Europe. *Holzforschung*, 74 (4), 333.

Moya, R., Berrocal, A., Rodriguez-Zuñiga, A., Vega-Baudrit, J. and Noguera, S. C. (2014a) Effect of silver nanoparticles on white-rot wood decay and some physical properties of three tropical wood species. *Wood and Fiber Science*, 46(4), 527–538.

Moya, R., Berrocal, A., Rodriguez-Zuñiga, A., Vega-Baudrit, J. and Noguera, S. C. (2014b) Effect of silver nanoparticles on white-rot wood decay and some physical properties of three tropical wood species. *Wood and Fiber Science*, 46(4), 527–538.

Moya, R., Gaitan-Alvarez, J., Berrocal, A. and Araya, F. (2020a) Effect of $CaCO_3$ in the wood properties of tropical hardwood species from fast-grown plantations in Costa Rica. *BioResources*, 15(3), 4802–4822.

Moya, R., Gaitan-Alvarez, J., Berrocal, A. and Araya, F. (2020b) Effect of $CaCO_3$ in the wood properties of tropical hardwood species from fast-grown plantations in Costa Rica. *Fresenius Environmental Bulletin*, 29(10), 9184–9194.

Moya, M., Leandro-Zúñiga, L. and Murillo-Gamboa, O. (2009) Wood characteristics of *Terminalia amazonia*, *Vochysia guatemalensis* and *Hyeronima alchorneoides* planted in Costa Rica. *Revista Bosque*, 30(2), 78–87.

Moya, R., Rodriguez-Zuñiga, A., Berrocal, A. and Vega-Baudrit, J. (2017) Effect of silver nanoparticles synthesized with NPsAg-ethylene glycol on brown decay and white decay fungi of nine tropical woods. *Journal of Nanoscience & Nanotechnology*, 17(8), 5233–5240.

Moya, R., Rodríguez-Zúñiga, A., Vega-Baudrit, J. and Álvarez, V. (2015) Effects of adding nano-clay (montmorillonite) on performance of polyvinyl acetate (PVAc) and urea-formaldehyde (UF) adhesives in *Carapa*

guianensis, a tropical species. *International Journal of Adhesion and Adhesives*, 59, 62–70.

Moya, R., Tenorio, C., Salas, J., Berrocal, A. and Muñoz, F. (2019) *Tecnología de la madera de plantaciones forestales. Editorial Tecnológica de Costa Rica*. 1st ed. (Cartago: Editorial Universidad de Costa Rica).

Nordstierna, L., Lande, S., Westin, M., Karlsson, O. and Furó, I. (2008) Towards novel wood-based materials: Chemical bonds between lignin-like model molecules and poly(furfuryl alcohol) studied by NMR. *Holzforschung*, 62(6), 709–713.

Oishi, S. S., Rezende, M. C., Origo, F. D., Damião, A. J. and Botelho, E. C. (2012) Viscosity, pH, and moisture effect in the porosity of poly(furfuryl alcohol). *Journal of Applied Polymer Science*, 128(3), 1680–1683.

Papadopoulos, A. N., Bikiaris, D. N., Mitropoulos, A. C. and Kyzas, G. Z. (2019) Nanomaterials and chemical modifications for enhanced key wood properties: A review. *Nanomaterials*, 9(4), 607.

Rahman, M. R., Lai, J. C. H. and Hamdan, S. (2018) Studies on the physical, mechanical, thermal and morphological properties of impregnated furfuryl alcohol-*co*-glycidyl methacrylate/nanoclay wood polymer nanocomposites. In *Wood Polymer Nanocomposites. Engineering Materials* (Cham: Springer), pp. 257–274. doi:10.1007/978-3-319-65735-6_14.

Rowell, R. M. (2012) *Handbook of Wood Chemistry and Wood Composites*. 2nd ed. (Boca Raton, FL: CRC Press, Taylor and Francis Group), pp. 703.

Rowell, R. M., Ibach, R. E., McSweeny, J. and Nilsson, T. (2009) Understanding decay resistance, dimensional stability and strength changes in heat treated and acetylated wood. *Wood Material Science and Engineering*, 1–2, 14–22.

Saka, S. (2000) Chemical composition and distribution. In D. N. S. Hon and N. Shiraishi (eds.) *Wood and Cellulosic Chemistry, Revised, and Expanded* (London: CRC Press), pp. 51–81.

Sandberg, D., Kutnar, A. and Mantanis, G. (2017) Wood modification technologies – a review. *iForest – Biogeosciences and Forestry*, 10(6), 895–908.

Sangregorio, A., Muralidhara, A., Guigo, N., Thygesen, L. G., Marlair, G., Angelici, C., de Jong, E. and Sbirrazzuoli, N. (2020) Humin based resin for wood modification and property improvement. *Green Chemistry*. doi:10.1039/c9gc03620b.

Schneider, M. H. (1995) New cell wall and cell lumen wood polymer composites. *Wood Science and Technology*, 29, 121–127.

Scott, N. and Chen, H. (2013) Nanoscale science and engineering for agriculture and food systems. *Industrial Biotechnology*, 9(1), 17–18.

Simon, C., Lion, C., Biot, C., Gierlinger, N. and Hawkins, S. (2018) Lignification and advances in lignin imaging in plant cell walls. In *Annual Plant Reviews Online* (NJ: Wiley), pp. 909–940.

Taghiyari, H. R., Bayani, S., Militz, H. and Papadopoulos, A. N. (2020b) Heat treatment of pine wood: possible effect of impregnation with silver nanosuspension. *Forests*, 11, 466. doi:10.3390/f11040466.

Taghiyari, H. R., Tajvidi, M., Taghiyari, R., Mantanis, G. I., Esmailpour, A. and Hosseinpourpia, R. (2020a) Chapter 19: Nanotechnology for wood quality improvement and protection. In *Nanomaterials for Agriculture and Forestry Applications*, pp. 469–489. doi:10.1016/B978-0-12-817852-2.00019-6.

Tarmian, A., Sepehr, A. and Gholamiyan, H. (2012) The use of nano-silver particles to determine the role of the reverse temperature gradient in moisture flow in wood during low-intensity conventive drying. *Special Topics and Reviews in Porous Media – An International Journal*, 3(2), 149–156.

Tarmian, A., Zahedi Tajrishi, I., Oladi, R. and Efhamisisi, D. (2020) Treatability of wood for pressure treatment processes: A literature review. *European Journal of Wood and Wood Products*, 78, 635–660.

Thygesen, L. G., Barsberg, S. and Venås, T. M. (2010) The fluorescence characteristics of furfurylated wood studied by fluorescence spectroscopy and confocal laser scanning microscopy. *Wood Science and Technology*, 44(1), 51–65.

Thygesen, L. G., Ehmcke, G., Barsberg, S. and Pilgård, A. (2020) Furfurylation result of Radiata pine depends on the solvent. *Wood Science and Technology*. doi:10.1007/s00226-020-01194-1.

Venås, T. M. and Rinnan, Å (2008) Determination of weight percent gain in solid wood modified with in situ cured furfuryl alcohol by near-infrared reflectance spectroscopy. *Chemometrics and Intelligent Laboratory Systems*, 92(2), 125–130.

Westin, M. (1996) *Development and evaluation of new alternative wood preservation treatments*. Final report to The Swedish Council for Forestry and Agri. Res. (SJFR) (in Swedish with an English summary), pp. 1–25.

Westin, M., Nilsson, T. and Hadi, Y. S. (1998) Field performance of furfuryl alcohol treated wood. In *Proceedings of the 4th Pacific rim bio-based composites symposium*, Bogor, Indonesia, pp. 305–331.

Xie, Y., Fu, Q., Wang, Q., Xiao, Z. and Militz, H. (2013) Effects of chemical modification on the mechanical properties of wood. *European Journal of Wood and Wood Products*, 71(4), 401–416.

Yang, T., Cao, J. and Ma, E. (2019) How does delignification influence the furfurylation of wood? *Industrial Crops and Products*, 135, 91–98.

Zhou, S., Xue, Y., Sharma, A. and Bai, X. (2016) Lignin valorization through thermochemical conversion: Comparison of hardwood, softwood and herbaceous lignin. *ACS Sustainable Chemistry and Engineering*, 4(12), 6608–6617.